American Mineralogist, Volume 93, pages 713–727, 2008

The crystal structure of vurroite, $Pb_{20}Sn_2(Bi,As)_{22}S_{54}Cl_6$: OD-character, polytypism, twinning, and modular description

Daniela Pinto,[1,*] Elena Bonaccorsi,[2] Tonci Balić-Žunić,[3] and Emil Makovicky[3]

[1]Dipartimento Geomineralogico, University of Bari, Via E. Orabona 4, I-70125 Bari, Italy
[2]Dipartimento di Scienze della Terra, University of Pisa, Via Santa Maria 53, I-56126 Pisa, Italy
[3]Department of Geography and Geology, University of Copenhagen, Østervoldgade 10, DK-1350 Copenhagen K, Denmark

Abstract

The crystal structure of the type specimen of vurroite from Vulcano (Aeolian Islands, Italy) has been solved and refined using single-crystal X-ray diffraction data collected at the Elettra synchrotron facility (Basovizza, Trieste). Vurroite has an OD (order-disorder) structure belonging to the category III of OD structures composed of equivalent layers. The OD-groupoid family (λ and σ partial operations) and MDO structures were derived by means of the application of the OD theory. The two theoretically possible polytypes with maximum degree of order (MDO polytypes) have pseudo-orthorhombic metric, with lattice parameters $a \approx 45.6$, $b \approx 8.4$, $c \approx 54$ Å, and $a \approx 22.8$, $b \approx 8.4$, $c \approx 54$ Å, and space group symmetries $F2/d11$ and $A2/d11$, respectively. Only the former polytype (MDO_1) could be identified in the analyzed crystals. The MDO_1 structure was solved and refined to $R = 6.26\%$ for 4968 reflections with $F_o > 4\sigma(F_o)$. In the standard $C2/c$ setting of the space group the unit-cell parameters of MDO_1 are $a = 8.371(2)$, $b = 45.502(9)$, $c = 27.273(6)$ Å, $\beta = 98.83(3)°$, $V = 10265(4)$ Å^3, $Z = 4$. Frequent twinning with (001) as the twin plane, together with the occurrence of disordered domains in the structure, was observed.

The crystal structure of vurroite contains lozenge-shaped composite rods made of coordination polyhedra of Pb and Sn, interconnected into layers parallel to (010) of the standard monoclinic setting. These layers are separated by ribbons of As and Bi, each in distorted octahedral coordination. The ribbons form wavy, discontinuous double layers of PbS archetype. Lone electron pairs of As and Bi are accommodated in the central portions of the PbS-like layers. The structure of vurroite contains building blocks topologically similar to those found in the zinckenite group and in the structure of kirkiite. It can be considered a box-work structure containing the smallest possible pseudo-hexagonal block in the form of a sole octahedron.

Keywords: Vurroite, Pb-Bi-As sulfosalts, crystal structure, OD-theory, polytypism, twinning

Introduction

Vurroite, a new Pb-Bi-As sulfosalt with the formula $Pb_{20}Sn_2(Bi,As)_{22}S_{54}Cl_6$, is a recently discovered mineral species named in honor of Filippo Vurro of the University of Bari (Garavelli et al. 2005). The mineral was found in fumarolic incrustations around high-temperature fumaroles at La Fossa crater of Vulcano, Aeolian Islands, Italy, where it is associated to the Pb-Bi-As sulfosalt kirkiite and several sulfides and sulfosalts of Pb and Bi. Vurroite occurs as slender, needle-shaped crystals up to 0.4 mm long and 0.01 mm across, which generally form fibrous aggregates.

In the present article, we describe the solution and refinement of the crystal structure of vurroite from the type locality. Its crystal-chemical characteristics, OD character, modular principles, and the relations with other sulfosalts are discussed.

Preliminary X-ray study

In a first attempt, a small fragment of vurroite ($0.0025 \times 0.01 \times 0.125$ mm) was measured using a Bruker AXS four-circle diffractometer equipped with CCD 1000 area detector (6.25×6.25 cm active detection-area, 512×512 pixels) and a flat graphite monochromator (Mo$K\alpha$ radiation from a fine-focus sealed X-ray tube). A total of 2800 frames were collected with an exposure time of 180 s per frame and crystal rotation 0.2° per frame. An orthorhombic primitive unit cell $a = 22.923(9)$, $b = 4.185(2)$, and $c = 27.04(2)$ Å was found, with data statistics and systematic absences suggesting a space group of the type *Pmmn*. A sound model of the crystal structure was found by direct methods (SHELXS program; Sheldrick 1997a), showing a high degree of chemical and positional disorder. However, the structure refinement did not converge to a satisfactory residual value, due to a very low average intensity of reflections, as well as to the high disorder present in the model of the crystal structure, which resulted in many overlapping atomic sites. Since the crystals were very small, a new intensity data collection was performed at the X-ray diffraction beamline XRD1, at the Elettra synchrotron facility (Basovizza-Trieste, Italy). The X-ray diffraction pattern of vurroite resulting from this experiment showed strong reflections pointing to the primitive orthorhombic sub-cell already obtained by the conventional single-crystal diffractometer, plus

* E-mail: d.pinto@geomin.uniba.it

a set of previously unobserved weaker reflections, which could be indexed by assuming a doubling of all of the three cell parameters. For this new orthorhombic super-cell with parameters a = 45.824(6), b = 8.368(2), c = 53.990(6) Å, V = 20702(6) Å^3, and Z = 8, the systematic absences indicated an F-centered lattice. As the diffraction pattern did not reveal any other reflection condition, the possible symmetries reduced to $F222$, $F2mm$, $Fm2m$, $Fmm2$, or $Fmmm$. After several trials, a reasonable structural model, conforming to the features of the initial one, was derived by direct methods in the space group $F2mm$ (SHELXS program; Sheldrick 1997a) and refined by successive least squares calculations and Fourier syntheses (SHELXL program; Sheldrick 1997b) to an acceptable R value (6.7%). However, some oddities in the obtained structural model were observed—the structure appeared composed of two alternating layers, the former being perfectly ordered, the latter interpreted as a superposition of two structures with partially occupied sites. The above evidence revealed the OD nature of the crystal structure of vurroite, which was the key element for the complete structural description of this mineral. Because of the important role played by the OD approach in the solution and refinement of the crystal structure of this complex sulfosalt, the next section will be devoted to the introduction of basic concepts of the OD theory, as well as to the description of the OD character of vurroite.

OD CHARACTER AND DERIVATION OF THE MDO POLYTYPES

OD structures are built up by one or more kinds of layers that can be stacked in two or more geometrically equivalent ways (Dornberger-Schiff 1956, 1964, 1966; Dornberger-Schiff and Fichtner 1972; see also Ďurovič 1997; Merlino 1997; Ferraris et al. 2004 for complete reviews of the OD theory). Whenever this occurs, an infinite number of possible distinct sequences of layers, ordered sequences (polytypes) as well as disordered sequences, may result. The full set of possible sequences forms a family of OD structures. For a complete description of an OD family presenting one kind of layer (as in vurroite), the metrics and symmetry of the OD layer, as well as the operations that convert a layer into the adjacent one, must be defined. The former are the so-called λ-symmetry operations, which form one of the 80 layer groups (Dornberger-Schiff 1959), whereas the latter are named σ-operations. Both of them are called partial operations (POs) in the OD terminology, since they are not necessarily valid for the whole crystal structure. They do not form a group, but a groupoid in the sense of Brandt (Dornberger-Schiff 1964).

All disordered and ordered sequences of the same OD-family display a common set of reflections, called family reflections, whereas they can be distinguished on the basis of the positions and intensities of additional "characteristic" reflections (non-family reflections). The family reflections are sharp, whereas the characteristic reflections may either be sharp or more or less diffuse, sometimes appearing as continuous streaks, depending on the degree of disorder in the stacking sequence. The family reflections do not depend on the stacking sequence, and correspond to a fictitious structure, periodic in three dimensions, formed by a superposition of individual layers in all possible positions corresponding to all the stacking vectors of the OD-family. This fictitious structure is called the "family structure" (or descriptively "average structure" or "sub-cell structure").

As a rule, deduction of the symmetry properties of the OD-family requires the knowledge of the OD layer, as well as of the symmetry operations that relate adjacent layers (σ-POs). They may often be obtained through a careful analysis of the diffraction pattern with attention to the systematic absences, both in the family reflections and in the diffraction pattern as a whole. The OD nature of vurroite, as well as its OD partial operations (λ- and σ-POs), were derived by looking at the observed structural arrangement as obtained in the space group $F2mm$. The crystal structure of vurroite belongs to the category III of OD structures composed of equivalent polar layers as defined in Dornberger-Schiff (1964), namely its λ-POs have τ character, whereas the σ-POs have ρ character (τ-POs do not reverse the layer, whereas ρ-POs do). Two other categories exist: category I presenting both λ- and σ-POs with τ and ρ character, and category II presenting λ- and σ-POs with only τ character. Whereas in OD structures of the first two categories pairs of adjacent layers are geometrically equivalent, in OD structures belonging to the category III a pair of consecutive layers (L_p; L_{p+1}) is equivalent to a pair of layers (L_q; L_{q+1}) only for values of p and q both even or both odd.

In the rest of this section, the orientations are given with respect to the previously described orthorhombic F-centered unit cell, with $a \approx 45.8$, $b \approx 8.4$, and $c \approx 54$ Å. The structure of vurroite consists of identical polar layers with symmetry $A(2)mm$ (here and in the following symmetry symbols, the parentheses indicate the direction of the missing periodicity), periodicities b ≈ 8.4, c ≈ 54, and width of the layer along the normal to (100) $a_0 \approx 11.4$ Å. As it happens in OD structures of category III, the layers succeed one another along the **a** direction with opposite sense of polarity; therefore, two distinct interlayer contacts alternate in this OD-structure (Fig. 1). The interlayer symmetry (σ-POs) consists of a glide plane n parallel to (100) with translation components ±¼**b** and ±¼**c** denoted as $n_{1/2,1/2}$ in the OD nomenclature (Dornberger-Schiff 1964; Ďurovič 1997), and twofold screw axes parallel to [010] and [001] with translation components ±¼**b** and ±¼**c**, respectively ($2_{1/2}$ in the OD nomenclature). The symbols used for the σ-POs are in keeping with those used in normal space group operations. In fact, "in n-fold screw operations the index gives, as usual, the number by which one has to multiply $1/n$ of the whole translation period or, if perpendicular to layers, of the layer distance to obtain the translational component. Similarly in axial glide operations, the index gives the number by which one has to multiply ½ of the period (or of the layer distance) to obtain the translational component" (Ďurovič 1997, p. 15).

The symbols of all the possible OD-groupoid families with monoclinic and orthorhombic symmetry are listed in Dornberger-Schiff and Fichtner (1972) and can be found also in Ferraris et al. (2004). The OD groupoid symbol for vurroite may be written as

A	(2)	m	m
	$\{(n_{1/2,1/2})$	$2_{1/2}$	$2_{1/2}\}$
	$\{(n_{1/2,1/2})$	$2_{1/2}$	$2_{1/2}\}$

where the first row indicates the λ-POs and the second and third rows indicate the σ-POs, which relate distinct pairs of layers in the structure. According to the above symbol, the polar layers with symmetry $A(2)mm$, periodicities $b \approx 8.4$, $c \approx 54$, and width $a_0 \approx 11.4$ Å follow one another along the direction normal to (100).

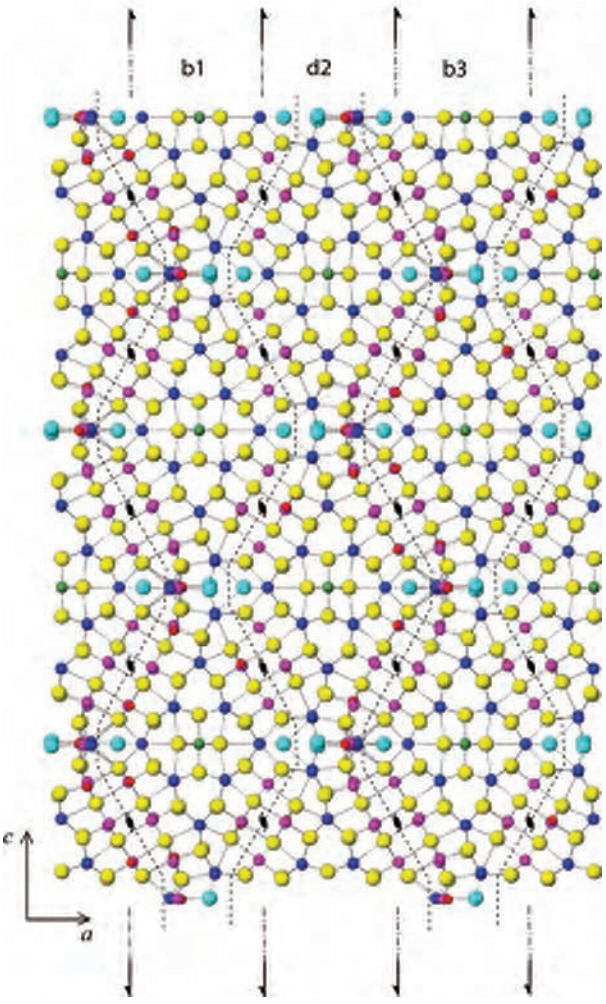

FIGURE 1. Representation of the σ partial symmetry operations in the crystal structure of vurroite (polytype MDO_1). The orientation of the pseudo-orthorhombic crystal axes (space group symmetry $F2/d11$) is indicated. The sequence of layers (b1, d2, b3) and partial symmetry operations ($n_{1/2,1/2}$, $n_{1/2,-1/2}$, $2_{1/2}$, and $2_{-1/2}$) are indicated. Yellow = S atoms; light blue = Cl atoms; pink = Bi atoms; blue = Pb atoms and Pb-dominated sites; red: = As atoms; green = (Sn,Bi) sites.

Each layer may be placed in two distinct positions with respect to the preceding one, either by the operation $n_{1/2,1/2}$ (glide plane normal to the **a** axis and with translation components +1/4 **b** and +1/4 **c**) or by the operation $n_{1/2,-1/2}$ (glide plane normal to the **a** axis and with translation components +1/4 **b** and –1/4 **c**). Due to the *A*-centering of the single OD layer, the application of the described $n_{1/2,1/2}$ operation is equivalent to the application of the operation $n_{-1/2,-1/2}$, whereas the application of the operation $n_{1/2,-1/2}$ is equivalent to the application of the operation $n_{-1/2,1/2}$.

An infinite number of stacking sequences is possible corresponding to the infinite number of possible sequences of operations $n_{1/2,1/2}$ and $n_{1/2,-1/2}$. Among the ordered structures, the OD theory pays particular attention to the so-called MDO polytypes (where MDO stands for "Maximum Degree of Order"), i.e., to the members of the OD-family "in which all layer triples, quadruples, etc., are geometrically equivalent or, at least, which contain the smallest possible number of *kinds* of those units" (Ďurovič 1997). A precise definition of MDO structures may be found in Dornberger-Schiff (1964) and in Ferraris et al. (2004).

This extended definition of MDO structures applies to vurroite, an OD structure belonging to category III. Two MDO polytypes exist for the vurroite OD-family: (1) MDO_1 (Fig. 2a), which is obtained by regularly alternating the application of the σ-operation $n_{1/2,1/2}$ and the operation $n_{1/2,-1/2}$. The resulting structure is metrically orthorhombic with unit-cell parameters $a_1 \approx 45.6$, $b_1 \approx 8.4$, and $c_1 \approx 54$ Å, but with monoclinic symmetry $F2/d11$. Transformed to a standard setting of the unit-cell it has the space group symbol $C2/c$ and cell parameters $a_1 \approx 8.4$, $b_1 \approx 45.6$, $c_1 \approx 27.3$, and $\beta_1 \approx 98.8°$ [transformation matrix: 010/100/0–½–½]; and (2) MDO_2 (Fig. 2b), which is obtained by the constant application of the σ-operation $n_{1/2,1/2}$. The same polytype is obtained by the constant application of the σ-operation $n_{-1/2,-1/2}$, whereas the constant application of the operation $n_{1/2,-1/2}$, as well as $n_{-1/2,1/2}$, gives rise to twin related MDO_2' structures. The MDO_2 polytype has pseudo-orthorhombic metric with cell parameters

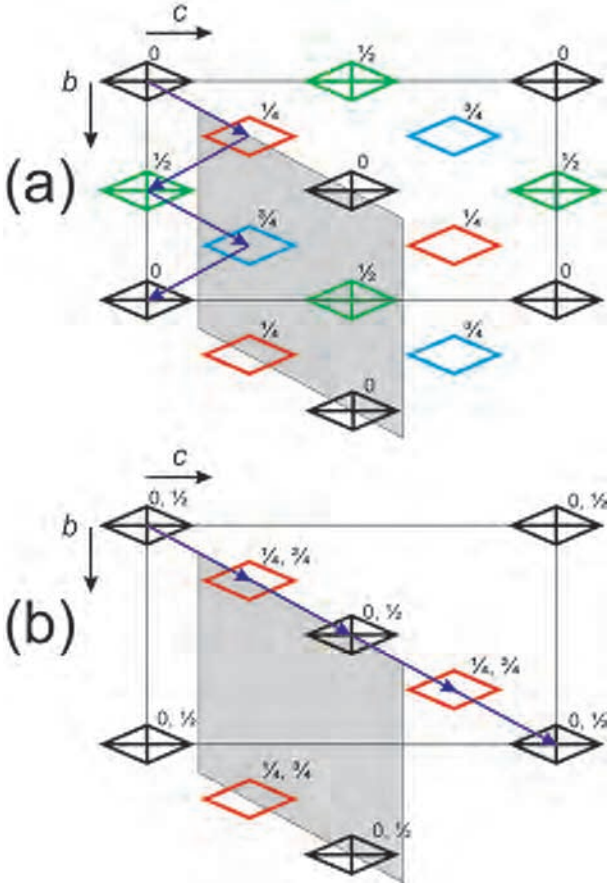

FIGURE 2. Schematic representation of the sequence of structural layers in the MDO polytypes of the vurroite family. The crystal-lattice directions **b** and **c** are referred to the pseudo-orthorhombic unit cell. The standard monoclinic unit cells are outlined in gray. The numbers indicate the levels, in parts of the ≈45.6 Å period, of structural layers that are parallel to the plane of projection. (**a**) Polytype MDO_1: pseudo-orthorhombic setting $F2/d11$, standard monoclinic $C12/c1$; (**b**) polytype MDO_2: pseudo-orthorhombic setting $A2/d11$, standard monoclinic $P12/c1$. Note that the origins of monoclinic unit cells are shifted to inversion centers at ⅛ *a*, ⅛ *b*, and ⅛ *c* of the pseudo-orthorhombic unit cell.

$a_2 \approx 22.8$, $b_2 \approx 8.4$, and $c_2 \approx 54$ and symmetry $A2/d11$. In the standard monoclinic setting, it has space group symmetry $P2/c$ and cell parameters $a_2 \approx 8.4$, $b_2 \approx 22.8$, $c_2 \approx 27.3$, and $\beta_2 \approx 98.8°$ [transformation matrix: 010/½00/0–½–½].

According to the nomenclature established by Guinier et al. (1984) the MDO_1 and MDO_2 polytypes should be denoted as vurroite-2*M* and vurroite-1*M*, respectively. Distinction can be made between the two polytypes through their diffraction pattern. The projection along **b*** of the reciprocal lattices of the two MDO polytypes are shown in Fig. 3. The family reflections correspond to the "family structure," with space group symmetry *Pmmn* and lattice parameters $a \approx 22.8$, $b \approx 4.2$, and $c \approx 27.3$ Å. Considering their pseudo-orthorhombic unit cells, the MDO_1 polytype of the vurroite family can be revealed by the occurrence of characteristic reflections with odd *h, k*, and *l* values (Fig. 3a), whereas the occurrence of reflections with odd *k* and *l* values, and a doubled *a** parameter, indicates the presence of the MDO_2 polytype (Fig. 3b).

Analysis of the diffraction patterns obtained at the Elettra synchrotron from several different crystals showed only maxima characteristic of the MDO_1 polytype of vurroite, suggesting that the polytype MDO_2 is not represented in the samples of vurroite from Vulcano (or at least is very rare). Moreover, it was observed that the characteristic MDO_1 reflections are slightly diffuse and have very weak intensities (Fig. 4). In some of the crystals examined only the family reflections could be observed.

The pseudo-orthorhombic crystal lattice and the possibility of stacking faults (connected to the OD nature of the structure) provides a basis for easy twinning in the MDO polytypes with (001) as the twin plane. This twin law corresponds to twinning by pseudo-merohedry with obliquity 0.04° for the MDO_1 polytype ($C2/c$ setting), and 0.05° for the MDO_2 polytype ($P2/c$ setting). Due to the practically orthorhombic metrics, the twinning could not be observed as a splitting of diffraction spots, but was confirmed by the structure refinement.

Single-crystal analysis of the polytype MDO_1 (vurroite-2*M*)

An exceptionally well-crystallized specimen of vurroite was found among samples collected in 1991 from the fumarole FF of the Vulcano fumarole field (T = 607 °C); it corresponds to the type specimen (Garavelli et al. 2005). The present structural study of vurroite-2*M* has been performed on a thin and well-crystallized crystal (size 0.003 × 0.010 × 0.110 mm) from this sample. The details about data collection and refinement are summarized in Table 1. The wavelength of the radiation was set to 1.0 Å and the crystal was placed at the distance of 40 mm from the 165 mm

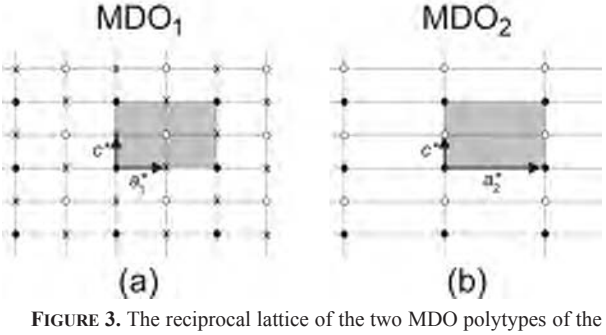

Figure 3. The reciprocal lattice of the two MDO polytypes of the vurroite family, as seen along b* of the pseudo-orthorhombic cell referred in the text. x = absent for any value of *k*; filled circle = present for $k = 2n$ (family reflections); open circle = present for $k = 2n+1$. The reciprocal unit cell of the family structure is shaded gray.

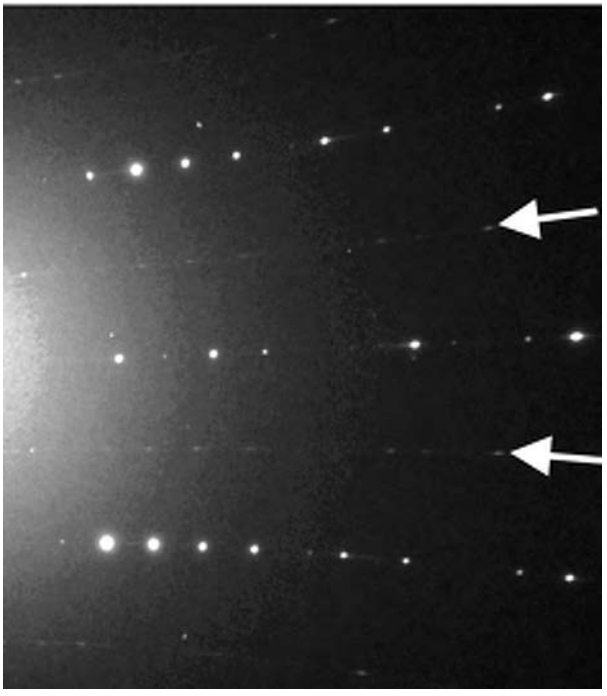

Figure 4. Diffraction pattern of vurroite collected with a CCD at the Elettra synchrotron facility. The arrows indicate rows of very weak and slightly diffuse reflections, corresponding to the MDO_1 polytype.

Table 1. Crystal data and summary of parameters describing data collection and refinement for vurroite

Crystal data	
Chemical formula (microprobe)	$Pb_{18.95}Sn_{1.30}(Bi_{12.99}As_{10.73}Tl_{0.03})_{\Sigma 23.75}(S_{54.71}Se_{0.22}Cl_{5.00}Br_{0.29})_{\Sigma 60.22}$
Chemical formula (diffraction)	$Pb_{19.20}Sn_{1.44}Bi_{13.94}As_{9.42}S_{54}Cl_6$
Crystal size (mm)	0.003 × 0.010 × 0.110
Cell setting, space group	Monoclinic, *C*2/*c*
a, *b*, *c* (Å); β (°)	8.371(2), 45.502(9), 27.273(6); 98.83(3)
V (Å^3)	10265(4)
Z	4
Dx (g/cm^3)	6.279
Data collection	
Radiation, λ	synchrotron, 1 Å
Temperature	293 K
Detector to sample distance	40 mm
Active detection-area	16.5 × 16.5 cm^2
Number of frames	93
Rotation width per frame	2°
Measuring time	dose = 150
Maximum observed 2θ	63.42 (*d* = 0.95 Å)
Unique reflections	5495
Reflections $I > 2\sigma_I$	4968
R_{int} after absorption correction	0.0319
R_σ	0.0423
Range of *h*, *k*, *l*	$-7 \le h \le 7$, $-45 \le k \le 46$, $-28 \le l \le 28$
Refinement	
$R[F_o > 4\sigma(F_o)]$	0.0626
R (all data)	0.0689
w*R* (on F_o^2)	0.1760
W*R* (all data)	0.1837
Goof	1.062
Number of least squares parameters	319

MarCCD detector. The 93 collected frames were obtained with a rotation angle $\Delta\phi = 2°$. Both family reflections and characteristic reflections of the polytype MDO_1 were recorded. Data reduction, including intensity integration, background and Lorenz polarization corrections, was carried out using the HKL software package (XDISP, DENZO, and SCALEPACK; Otwinowsky and Minor 1997). The preliminary model of the structure was obtained by applying direct methods (SHELXS-97 program; Sheldrick 1997a) in the space group *F*2*mm*, and then the atomic coordinates were transformed in the standard setting of the monoclinic space group *C*2/*c*, in accordance with the symmetry of the model provided by the OD theory, and assuming that twinning occurred. The structure refinement confirmed the (001) twinning with the twin ratio 1:1, which suggests the occurrence of frequent stacking faults, giving rise to polysynthetic twinning.

Positions of all metal and semimetal atoms were revealed by direct methods, whereas sulfur atoms were found in difference-Fourier maps during the subsequent refinements of the structure by full-matrix least squares based on F^2 (SHELXL-97 program; Sheldrick 1997b). For the correct assignment of atoms in the structure, interatomic distances and heights of maxima in Fourier maps were considered. In the beginning of the refinement 11 Pb sites were identified. Successive analysis of their coordination characteristics and bond valence calculations (Brese and O'Keeffe 1991) suggested mixed (Pb,Bi) occupancy for sites 7 and 8. In these sites, the occupancies of Pb and Bi were fixed on the basis of the results of the coordination analysis, and no refinement was attempted because of the negligible difference in the scattering powers of the two elements.

A relatively elongated displacement ellipsoid was found for site 11. This site could be split into three closely spaced sites that were attributed to Pb, Bi, and As, respectively, on the basis of the shortest distances to sulfur atoms. The three atomic species were refined with equal and isotropic displacement parameters and the sum of occupancies was constrained to 1, but the coordinates were kept independent. The resulting coordinations for Pb11, Bi11, and As11 are in agreement with the values expected for Pb, Bi, and As atoms, respectively.

The cation sites M12 and M13 (Fig. 5) were first considered to be the pure Sn sites. Refinements with free occupancy factors for these cation sites showed electron densities intermediate between those of Bi(Pb) and Sn(As). Crystal-chemical considerations and the final values of bond-lengths indicated M12 and M13 to be mixed Sn/Bi sites. According to the Fourier maps, the Sn(Bi) sites were split into two symmetrically related sites lying close to the twofold axes, and therefore no further splitting into independent Sn and Bi sites was attempted. Because the two close sites cannot be simultaneously occupied, they represent a statistical deviation of cations from the center of the coordination polyhedron due to the lone electron pair activity (Bi) or to a small size of the cation relative to the size of the polyhedron (Sn). The symmetry is therefore decreased locally to *Cc* due to the deviation of Sn(Bi) from the symmetry axis. Inside one column of octahedra, one could expect that the cations might all be displaced in one direction (either "up" or "down" the monoclinic [100]). Various senses of displacement inside the same column, in fact, would inevitably lead to the overbonding of some S atoms, and the underbonding of others. However, the refinement in the non-centrosymmetric space group *Cc* did not improve the results of refinement, suggesting that the displacements in different columns are unrelated, and happen with equal probability and a statistical distribution through the structure. The final refinement was therefore made in space group *C*2/*c*. Refinement of Sn(Bi) mixed positions gave site occupation factors 0.36(1) Sn and 0.14(1) Bi for both the sites M12 and M13. The total content of Sn so obtained is 1.44 apfu, which is in good agreement with microprobe data of 1.30 apfu (Table 1). In the refinement, Sn and Bi coordinates, as well as the isotropic displacement parameters, were constrained to be identical and the occupancies were constrained to the total of one.

On the basis of bond-valence calculations and bond-lengths, Sn was estimated to be tetravalent in the structure of vurroite; this has been confirmed by the balance of valences in the final crystal-chemical formula (Garavelli et al. 2005).

It was found during the refinement that the family reflections are considerably stronger than the resulting ordered crystal structure justifies. This is explained as a presence in the crystal of a considerable percentage of fully disordered domains, mixed with the domains of ordered structure of the MDO_1 polytype. To eliminate the contribution of the disordered portions ("Ďurovič effect;" Nespolo and Ferraris 2001), separate scale factors were assigned to the group of family and the group of characteristic reflections, respectively. The relative scale factors were varied in regular increments of 0.10 and the resulting *R* values from the structure refinements were compared. The minimum value of the reliability *R* index was reached when the relative scale factor for the family reflections was 0.5, which indicates that the ordered domains of the MDO_1 polytype represent ~50% of the crystal volume.

Before the introduction of the separate scale factors for the family and characteristic reflections, the sites M16–M23 (Table 2) showed distances to sulfur atoms and electron densities suggesting a mixed (As,Bi) occupancy. With the application of different scale factors for the two groups of reflections, it was possible to define most of them as either pure Bi or As sites. This indicates that the previously suggested chemical disorder does not actually occur, and is due to the presence of stacking disorder in a large part of the crystal (~50% in volume). Only the sites M18, M20, and M22 remain with mixed characteristics after the introduction of two different scale factors, suggesting that in these sites atomic substitutions really take place inside the MDO_1-ordered domains. These mixed (As,Bi) sites were finally refined with identical isotropic displacement factors, and their coordinates were not constrained, but the sums of the occupancies for each As + Bi pair were constrained to 1.

As the scattering factors of S and Cl are very close, bond-valence calculations were used for the identification of Cl among the anion sites. This allowed identifying three sites that were at least preferentially occupied by Cl anions (Cl1, Cl2, and Cl3). In accordance with the final valence-balanced chemical formula of vurroite derived from the microprobe measurements (Garavelli et al. 2005), an additional amount of Cl (about 2 apfu) should be distributed over the remaining S sites. For all S and Cl atoms, isotropic displacement parameters were used in the refinement.

The final structure refinement, which also included the two twin components, converged to $R = 0.0626$ [4968 reflections with

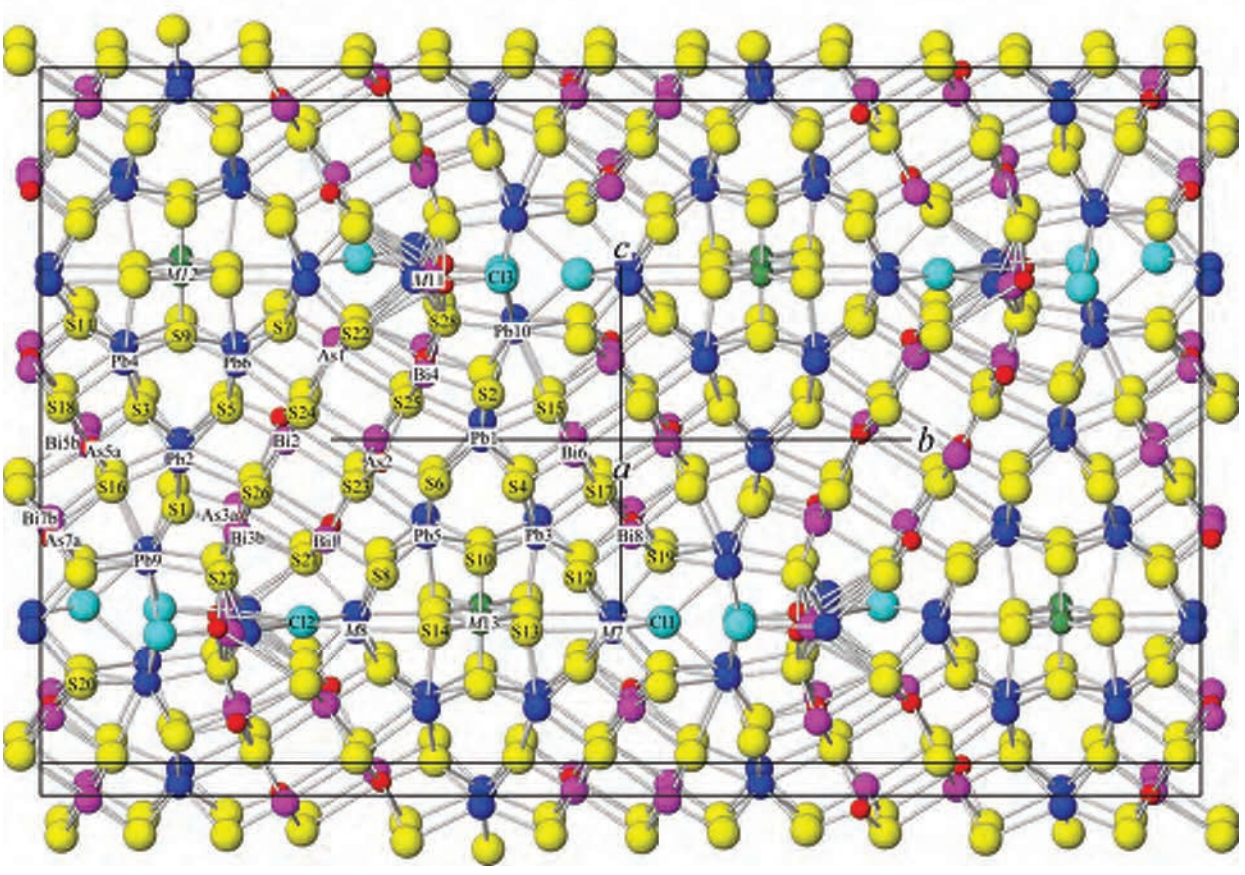

FIGURE 5. The crystal structure of the polytype MDO_1 (vurroite-2*M*) of the vurroite family in the standard monoclinic setting, space group symmetry *C*12/*c*1, and cell parameters $a = 8.371(2)$, $b = 45.502(9)$, $c = 27.273(6)$ Å, and $\beta = 98.83(3)°$ projected on (100). Color codes as in Figure 1.

$I > 2\sigma(I)$]. Fractional atomic coordinates, occupation factors and displacement parameters are shown in Table 2. Table 3[1] lists the observed and calculated structure factors, while selected bond distances are shown in Table 4. Coordination parameters for cations are summarized in Table 5.

DESCRIPTION OF THE STRUCTURE

General description

In the following paragraph, the directions are specified in terms of the standard *C*12/*c*1 setting of the space group. The crystal structure of vurroite is built of trigonal rods comprising three edge-connected [100] columns of base-sharing [PbS_6] trigonal prisms. In the following, trigonal prisms oriented parallel to [100] are designated as "standing" prisms, and those oriented perpendicular to [100] are designated "lying" prisms. Two such rods and two [100] columns of lying [(Pb,Bi)S_6] trigonal prisms surround a single column of the edge-sharing [(Sn,Bi)S_6] coordination octahedra. The resulting lozenge-shaped composite rods are surrounded by ribbons of coordination pyramids of As and Bi with trapezoidal bases and apical vertices oriented toward the rods (Fig. 6). The ribbons on the opposing sides of the lozenges are respectively two and three pyramids wide (ribbons 2R and 3R, respectively). They conform to the general PbS archetype in orientation toward the equivalent ribbons facing them from the surfaces of the adjacent lozenges. Consequently, the lozenge-shaped rods are separated by wavy, discontinuous double-layers of PbS archetype (with As and Bi as cations), completed by the rods of lying trigonal prisms of M7, M8, and M11 on the ¼ and ¾ *z* levels (Figs. 5 and 7). The straight portions of PbS-like layers formed of 2R and 3R ribbons on the opposing sides of the lozenges, are denoted C and D rods, respectively, in the following. The lone electron pairs of As and Bi are accommodated in the central spaces of the PbS-like layers.

Lozenge-shaped rods

The main elements of the lozenge-shaped rods are the standing bi-capped trigonal prisms of Pb clustered around a partial threefold axis (Fig. 6). This triangular cluster consists of six independent cation sites (M1–M6) alternating in pairs along

[1] Deposit item AM-08-023, Table 3 (observed and calculated structure factors). Deposit items are available two ways: For a paper copy contact the Business Office of the Mineralogical Society of America (see inside front cover of recent issue) for price information. For an electronic copy visit the MSA web site at http://www.minsocam.org, go to the American Mineralogist Contents, find the table of contents for the specific volume/issue wanted, and then click on the deposit link there.

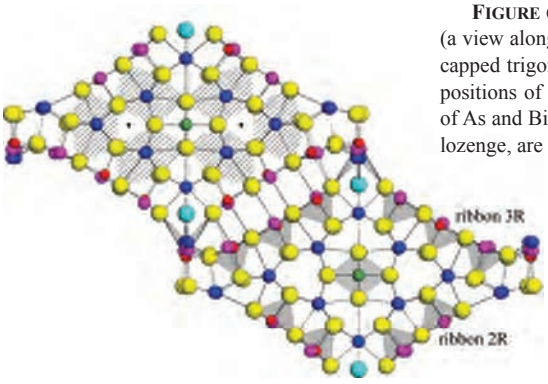

FIGURE 6. Lozenge-shaped rods in the crystal structure of vurroite (a view along [100]). In the upper left lozenge, the trigonal rods of bi-capped trigonal prisms of Pb (hatched) are outlined, and dots indicate positions of partial threefold axes. Ribbons of coordination pyramids of As and Bi, as well as the [(Sn,Bi)S_6] octahedron in the center of the lozenge, are shaded gray in the lower right lozenge.

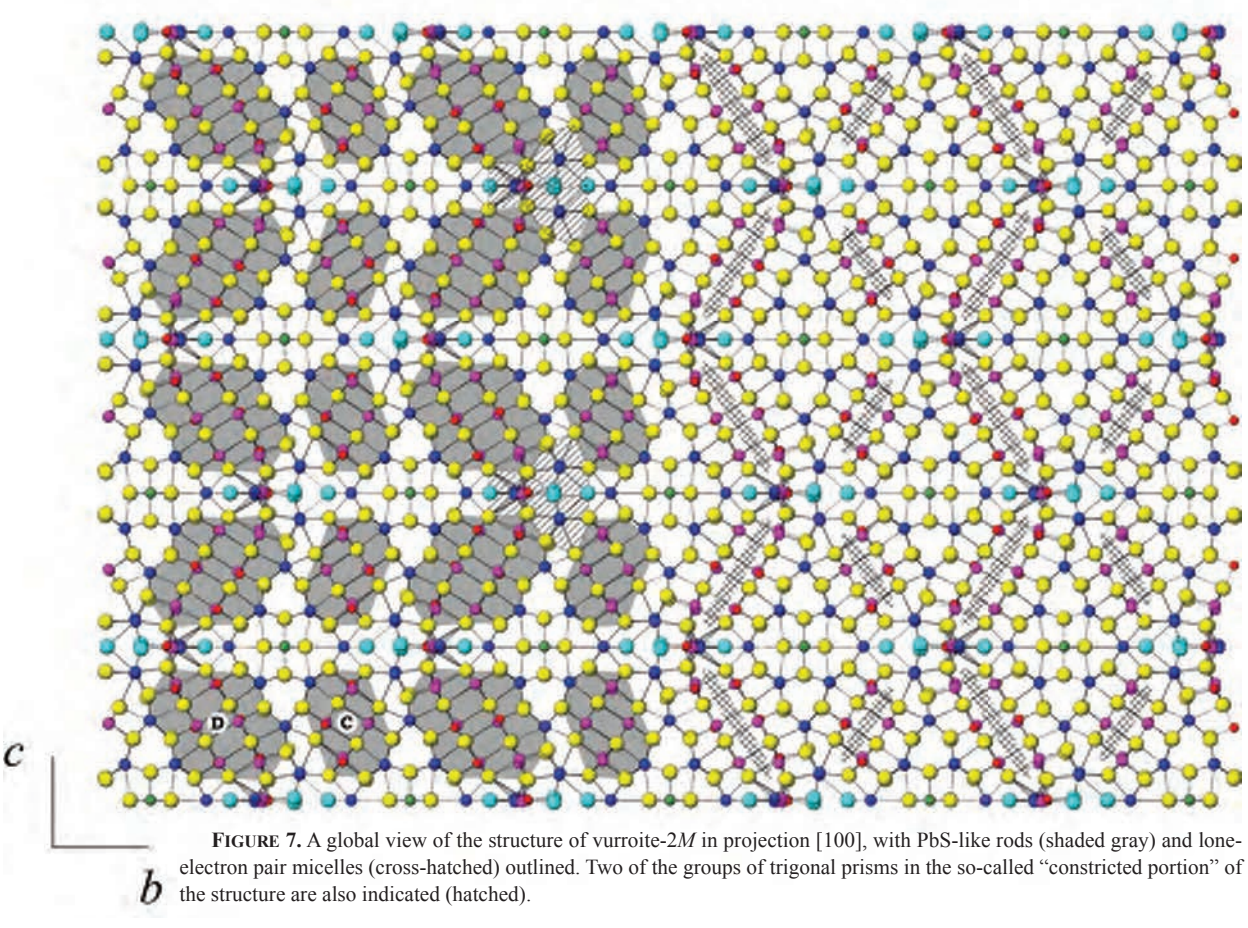

FIGURE 7. A global view of the structure of vurroite-2*M* in projection [100], with PbS-like rods (shaded gray) and lone-electron pair micelles (cross-hatched) outlined. Two of the groups of trigonal prisms in the so-called "constricted portion" of the structure are also indicated (hatched).

[100] columns. The coordination environment and M-S distances are characteristic for Pb atoms. The distances of Pb atoms to the capping S atoms from the ribbon 3R are distinctly longer than to those from the ribbon 2R (Fig. 6).

The triangular clusters are connected by a layer formed by a central [100] column of alternating M12 and M13 octahedra flanked by two columns of lying trigonal prisms (M7 and M8) (Figs. 5 and 6). The sites M12 and M13 show very eccentric octahedral coordination (Fig. 8). The distances of the central cation to the octahedral vertices in the direction perpendicular to (001) are 2.479(16) Å and 2.494(16) Å for M12, 2.492(13) Å and 2.512(14) Å for M13. In the MeS_4 plane (001), the ratio Me-S13/Me-S14 between pairs of opposing bonds is respectively 2.487(10)/2.878(11) and 2.854(11)/2.510(11) for M12, and 2.585(10)/3.088(11) and 3.113(10)/2.559(11) for M13.

The high eccentricity of the cations M12 and M13, unusual for tetravalent Sn, is connected to the Bi for Sn substitution in these sites. The eccentricity of Bi can be explained by the stereo chemical activity of its lone electron pair, whereas the eccentric position of Sn is a result of its small size in comparison with the size of the octahedral void. The average octahedral Sn^{IV}-S distance (2.577) in levyclaudite (Evain et al. 2006) and (2.572) in SnS_2 (Palosz and

TABLE 2. Atom coordinates, displacement parameters, and occupancies for vurroite

Site	Atom	s.o.f.	*x*	*y*	*z*	U_{11}	U_{22}	U_{33}	U_{23}	U_{13}	U_{12}	U_{eq}
M1	Pb1	1	0.3838(4)	0.12038(4)	0.50934(6)	0.045(1)	0.059(1)	0.0410(9)	–0.0032(7)	0.003(2)	0.006(2)	0.0486(5)
M2	Pb2	1	0.8798(4)	0.11928(4)	0.50973(6)	0.049(1)	0.060(1)	0.0428(9)	–0.0049(8)	0.004(2)	0.013(2)	0.0507(5)
M3	Pb3	1	0.3037(4)	0.07225(4)	0.36465(7)	0.045(1)	0.049(1)	0.077(1)	–0.0146(9)	0.006(2)	–0.0009(15)	0.0577(5)
M4	Pb4	1	0.8105(4)	0.07164(4)	0.36639(7)	0.045(1)	0.049(1)	0.069(1)	–0.013(9)	0.003(2)	–0.002(2)	0.0552(5)
M5	Pb5	1	0.3094(4)	0.16778(4)	0.36618(7)	0.050(1)	0.050(1)	0.072(1)	0.0202(9)	0.013(2)	–0.001(2)	0.0567(5)
M6	Pb6	1	0.8079(4)	0.16868(4)	0.36905(7)	0.046(1)	0.050(1)	0.078(1)	0.0238(9)	0.008(2)	–0.003(2)	0.0581(5)
M7	Pb7	0.80*	0.7387(3)	0.99299(4)	0.74970(7)	0.040(1)	0.097(1)	0.0457(8)	–0.003(1)	0.008(2)	–0.014(1)	0.0607(5)
	Bi7′	0.20*	0.7387(3)	0.99299(4)	0.74970(7)	0.040(1)	0.097(1)	0.0457(8)	–0.003(1)	0.008(2)	–0.014(1)	0.0607(5)
M8	Pb8	0.60*	0.7385(2)	0.22831(3)	0.25004(6)	0.038(1)	0.0541(9)	0.0396(7)	–0.0007(8)	0.007(2)	–0.0054(8)	0.0437(4)
	Bi8′	0.40*	0.7385(2)	0.22831(3)	0.25004(6)	0.038(1)	0.0541(9)	0.0396(7)	–0.0007(8)	0.007(2)	–0.0054(8)	0.0437(4)
M9	Pb9	1	0.9617(4)	0.09124(4)	0.66089(7)	0.049(1)	0.065(1)	0.060(1)	0.0076(9)	0.006(1)	–0.006(2)	0.0583(5)
M10	Pb10	1	0.4553(5)	0.09208(5)	0.6680(1)	0.077(2)	0.076(1)	0.1140(2)	–0.010(1)	0.041(2)	–0.002(2)	0.0845(7)
M11	PB11	0.2	0.2326(9)	0.1776(2)	0.7445(2)	0.0241(8)						
	BI11	0.3	0.2396(7)	0.1635(1)	0.7444(2)	0.0241(8)						
	As11	0.5	0.244(1)	0.1524(2)	0.7521(3)	0.0241(8)						
M12	Sn1a	0.36(1)	0.0295(7)	0.12079(8)	0.2499(5)	0.042(2)						
	Bi1b	0.14(1)	0.0295(7)	0.12079(8)	0.2499(5)	0.042(2)						
M13	Sn2a	0.36(1)	0.5409(5)	0.12114(8)	0.2501(4)	0.040(2)						
	Bi2b	0.14(1)	0.5409(5)	0.12114(8)	0.2501(4)	0.040(2)						
M14	Bi1	1	0.5606(4)	0.25453(4)	0.37186(5)	0.036(1)	0.0406(9)	0.0411(8)	–0.0070(6)	0.009(1)	–0.006(1)	0.0387(4)
M15	As1	1	0.4301(9)	0.25011(9)	0.6298(2)	0.031(3)	0.028(3)	0.054(3)	–0.001(2)	0.010(3)	0.007(3)	0.037(1)
M16	Bi2	1	0.1190(4)	0.21064(5)	0.49487(6)	0.049(1)	0.088(1)	0.0438(9)	–0.0017(8)	0.013(1)	–0.005(2)	0.0594(5)
M17	As2	1	0.6252(9)	0.20655(7)	0.4864(2)	0.031(3)	0.017(2)	0.047(2)	0.006(2)	0.023(3)	0.006(3)	0.0299(9)
M18	As3a	0.81(1)	0.195(1)	0.1689(1)	0.6129(3)	0.025(1)						
	Bi3b	0.19(1)	0.194(2)	0.1696(2)	0.6289(4)	0.025(1)						
M19	Bi4	1	0.6726(5)	0.16939(5)	0.61481(7)	0.057(1)	0.079(1)	0.054(1)	–0.0108(9)	0.006(1)	–0.010(1)	0.0632(6)
M20	As5a	0.62(1)	0.131(4)	0.0434(4)	0.5049(6)	0.045(1)						
	Bi5b	0.38(1)	0.128(3)	0.0411(2)	0.4997(4)	0.045(1)						
M21	Bi6	1	0.6265(4)	0.04028(4)	0.49896(5)	0.048(1)	0.0405(9)	0.0435(9)	–0.0005(6)	0.010(1)	–0.002(1)	0.0437(5)
M22	As7a	0.78(1)	0.930(1)	0.0088(1)	0.6278(3)	0.028(1)						
	Bi7b	0.22(1)	0.947(1)	0.009(2)	0.6114(4)	0.028(1)						
M23	Bi8	1	0.4306(4)	0.00887(4)	0.62198(6)	0.052(1)	0.060(1)	0.0454(9)	0.0066(8)	–0.003(1)	0.003(1)	0.0536(5)
	S1	1	0.172(2)	0.1181(2)	0.5939(3)	0.029(2)						
	S2	1	0.664(2)	0.1147(2)	0.5847(3)	0.032(2)						
	S3	1	0.096(2)	0.0854(2)	0.4484(3)	0.030(2)						
	S4	1	0.600(2)	0.0885(2)	0.4509(3)	0.027(2)						
	S5	1	0.105(2)	0.1603(2)	0.4476(3)	0.019(2)						
	S6	1	0.609(2)	0.1603(2)	0.4556(3)	0.031(2)						
	S7	1	0.456(2)	0.2929(2)	0.6726(3)	0.028(2)						
	S8	1	0.542(2)	0.2059(2)	0.3204(3)	0.023(2)						
	S9	1	0.040(2)	0.1209(2)	0.3418(3)	0.029(2)						
	S10	1	0.535(2)	0.1213(2)	0.3419(3)	0.033(2)						
	S11	1	0.044(2)	0.0338(2)	0.3236(3)	0.032(2)						
	S12	1	0.460(2)	0.9647(2)	0.6828(3)	0.027(2)						
	S13	1	0.763(1)	0.0817(2)	0.2498(3)	0.034(2)						
	S14	1	0.760(1)	0.1602(2)	0.2492(4)	0.035(2)						
	S15	1	0.369(1)	0.0606(2)	0.5512(3)	0.031(2)						
	S16	1	0.935(1)	0.0615(2)	0.5523(3)	0.035(3)						
	S17	1	0.621(1)	0.9818(2)	0.5659(3)	0.038(3)						
	S18	1	0.808(1)	0.0180(2)	0.4326(3)	0.026(2)						
	S19	1	0.756(1)	0.0350(2)	0.6684(4)	0.040(3)						
	S20	1	0.160(1)	0.0345(2)	0.6696(4)	0.035(3)						
	S21	1	0.263(1)	0.2285(2)	0.6726(3)	0.026(2)						
	S22	1	0.660(1)	0.2280(2)	0.6722(3)	0.028(2)						
	S23	1	0.392(1)	0.2273(2)	0.4410(3)	0.030(2)						
	S24	1	0.798(1)	0.2259(2)	0.4406(3)	0.028(2)						
	S25	1	0.358(1)	0.1844(2)	0.5599(3)	0.032(3)						
	S26	1	0.952(1)	0.1856(2)	0.5605(3)	0.031(2)						
	S27	1	0.926(1)	0.1563(2)	0.6817(3)	0.034(3)						
	S28	1	0.508(1)	0.1526(2)	0.6830(3)	0.031(2)						
	Cl1†	1	0.5	0.0372(2)	0.75	0.032(3)						
	Cl2†	1	0	0.2259(3)	0.75	0.034(3)						
	Cl3†	1	0.2420(1)	0.1024(2)	0.7423(3)	0.029(2)						

Note: In accordance with the chemical analysis and the valence balance, two additional Cl apfu should be distributed over sites labeled S (this gives an average of about 3.5% Cl in each S site).

* Occupancies estimated from a crystal chemical analysis (see the text).

† Assumed in accordance with the results of bond–valence calculations (Brese and O'Keeffe 1991); they correspond to 4 Cl apfu.

Salje 1989) should be compared to the average bond lengths of M12 and M13 (2.62 and 2.73 Å, respectively; Table 5).

The closest caps of the polyhedra around M7 and M8 are Cl atoms (Cl1 and Cl2, respectively), while the farthest ones are sulfur atoms that are shared with the adjacent octahedra M12 and M13.

Trapezoidal ribbons

On the two opposite sides of the lozenge-shaped rods, the repetition along [100] of the pyramidally coordinated polyhedra forms trapezoidal ribbons with the thickness of two (2R) and three (3R) trapezoids, respectively (Fig. 9).

The pure arsenic positions As1 and As2 show a very typical

TABLE 4. Selected interatomic distances (Å) for vurroite

Pb1-S2	2.881(12)	Pb2-S16	2.883(9)	Pb3-S11	2.883(12)
-S15	2.961(9)	-S2	2.939(14)	-S12	3.031(12)
-S4	2.966(13)	-S4	2.980(13)	-S10	3.081(13)
-S1	3.117(13)	-S3	3.063(13)	-S17	3.105(9)
-S6	3.140(12)	-S1	3.089(12)	-S13	3.115(8)
-S3	3.141(13)	-S6	3.126(12)	-S9	3.120(13)
-S5	3.222(10)	-S5	3.298(11)	-S3	3.133(13)
-S25	3.244(9)	-S26	3.336(9)	-S4	3.229(12)
Pb4-S12	2.954(11)	Pb5-S7	2.918(12)	Pb6-S8	2.942(11)
-S11	2.973(13)	-S10	2.976(13)	-S7	2.994(13)
-S18	3.039(8)	-S8	3.020(12)	-S5	3.045(11)
-S3	3.076(13)	-S5	3.025(12)	-S9	3.083(13)
-S9	3.091(13)	-S9	3.102(13)	-S6	3.113(12)
-S13	3.176(8)	-S14	3.130(11)	-S10	3.144(13)
-S4	3.204(13)	-S6	3.237(12)	-S14	3.254(11)
-S10	3.226(13)	-S23	3.394(9)	-S24	3.263(9)
Pb7-CL1	2.836(7)	Pb8-CL2	2.886(7)	Pb9-S1	2.988(13)
-S20	2.923(10)	-S8	2.895(12)	-CL3	3.015(9)
-S19	2.948(11)	-S21	2.915(9)	-S27	3.037(9)
-S12	2.961(12)	-S22	2.935(9)	-S20	3.062(10)
-S12	3.021(11)	-S8	2.980(11)	-S19	3.109(10)
-S11	3.149(12)	-S14	3.104(8)	-S2	3.177(12)
-S11	3.237(12)	-S7	3.141(12)	-S16	3.233(9)
-S13	3.404(8)	-S7	3.207(12)	-CL3	3.394(10)
Pb10-S28	2.809(9)	Pb11-S27	2.752(12)	Bi11-S27	2.637(11)
-CL3	2.937(10)	-S28	2.932(11)	-S28	2.710(10)
-S1	3.102(12)	-CL2	2.957(10)	-CL3	2.783(9)
-S2	3.236(13)	-S27	3.016(12)	-S27	2.922(11)
-CL3	3.275(9)	-S21	3.072(11)	-S28	3.043(12)
-CL1	3.335(7)	-S28	3.256(12)	-CL2	3.493(9)
-S15	3.467(9)	-S22	3.257(11)	-S21	3.569(10)
-S20	3.611(10)	-CL3	3.423(10)	-S22	3.728(10)
-S19	3.615(11)				
As11-CL3	2.293(10)	Sn1a/Bi1b-S9	2.479(16)	Sn2a/Bi2b-S10	2.492(13)
-S27	2.471(13)	-S13	2.487(10)	-S10	2.512(14)
-S28	2.514(12)	-S9	2.494(16)	-S14	2.559(11)
-S27	3.037(12)	-S14	2.510(11)	-S13	2.585(10)
-S28	3.117(13)	-S13	2.854(11)	-S14	3.088(11)
-CL2	3.913(11)	-S14	2.878(11)	-S13	3.113(10)
-S21	4.101(12)				
-S22	4.028(12)				
Bi1-S8	2.613(8)	As1-S21	2.188(11)	Bi2-S5	2.623(8)
-S23	2.813(10)	-S7	2.263(9)	-S26	2.689(10)
-S24	2.831(9)	-S22	2.319(11)	-S25	2.736(9)
-S21	2.897(9)	-S23	3.235(10)	-S24	2.946(9)
-S22	2.898(10)	-S24	3.377(11)	-S23	2.997(10)
-S26	3.301(9)	-S25	3.548(10)	-S23	3.334(9)
As2-S24	2.232(11)	As3a-S25	2.252(13)	Bi3b-S1	2.526(12)
-S6	2.262(9)	-S1	2.369(10)	-S25	2.584(16)
-S23	2.342(10)	-S26	2.421(12)	-S26	2.638(15)
-S26	3.282(11)	-S28	3.090(12)	-S27	2.907(18)
-S25	3.378(12)	-S21	3.172(11)	-S28	2.915(16)
-S24	3.665(9)	-S27	3.191(14)	-S21	2.955(12)
Bi4-S28	2.594(10)	As5a-S15	2.323(29)	Bi5b-S15	2.438(22)
-S2	2.619(9)	-S16	2.385(31)	-S3	2.445(12)
-S27	2.646(10)	-S3	2.447(19)	-S16	2.496(23)
-S25	2.904(10)	-S17	3.248(30)	-S17	3.136(24)
-S26	3.044(11)	-S18	3.267(20)	-S18	3.184(22)
-S22	3.102(9)	-S18	3.302(28)	-S18	3.259(13)
Bi6-S4	2.548(8)	As7a-S19	2.293(14)	Bi7b-S20	2.484(14)
-S17	2.703(10)	-S11	2.336(10)	-S11	2.625(12)
-S18	2.729(10)	-S20	2.388(13)	-S19	2.670(16)
-S15	2.914(11)	-S17	3.112(14)	-S18	2.817(15)
-S16	2.929(11)	-S16	3.168(11)	-S16	2.875(12)
-S17	3.235(9)	-S18	3.185(14)	-S17	3.076(15)
Bi8-S12	2.592(8)				
-S18	2.603(9)				
-S17	2.677(11)				
-S20	3.013(11)				
-S15	3.037(9)				
-S19	3.062(11)				

pyramidal coordination As_{3+2} with the short As-S distance to the apex of the pyramid equal to 2.263(9) and 2.262(9) Å, respectively, and the two pairs of opposing bonds in the base of the pyramid being respectively short [from 2.188(11) to 2.342(10) Å] and long [from 3.235(10) to 3.378(11) Å]. The pure Bi positions (Bi1, Bi2, Bi4, Bi6, and Bi8) are characterized by short Bi-S distances in the base of the pyramid, which range from 2.603(10) to 2.813(10), and longer Bi-S distances ranging from 2.898(10) to 3.044(11) Å. The distances of the central Bi atoms to the apices of the pyramids range from 2.548(8) to 2.623(8) Å. It can be seen (Table 4) that the three shortest bonds in the Bi1 coordination polyhedron are relatively long compared with the other Bi sites. This suggests a possible presence of Pb in this site, which seems to be further confirmed by a relatively small S23-Bi1-S24 angle (~74°), indicating a shift of the cation in the base of the pyramid.

In Figure 10, the element-specific bond-length hyperbolae taken from Berlepsch et al. (2001) are reported, with M-S distances for pyramidally coordinated As and Bi sites in vurroite added. Pairs of M-S distances in the base of the pyramids are plotted in the space above the median line, whereas the pairs of opposing bonds perpendicular to the base of the pyramids are plotted in the space below this line (they represent respectively the short bond to the apex of the pyramids and the long weak M-S distances that straddle the lone electron pairs in the interspaces of the PbS-like layer). The diagram shows that cation-to-ligand distances of As and Bi coordination polyhedra plot close to the As or the Bi curves in agreement with the refined occupancies. Deviations were observed for the mixed sites M18 (As3a, Bi3b), M20 (As5a, Bi5b), and M22 (As7a, Bi7b). Additionally, the Bi1 pairs of bond lengths in the base of the pyramid plot between the Bi and Pb curves. This again gives an indication of the mixed (Pb,Bi) character of Bi1.

As can be seen on Figure 9, the Bi sites in 3R ribbons alternate with pure As or As-dominated sites both along the extension of a ribbon ([100]) and in the direction perpendicular to it, whereas in 2R ribbons they alternate along [100], but the same type of cation sites are paired in the perpendicular direction. In the 3R ribbons, the ordering of Bi and As in every second coordination polyhedron is almost complete, with mixing only in the marginal As-dominated site M18. In the 2R ribbon, both As-dominated sites (M20 and M22) have also Bi contents that are larger than that found in M18. This shows that 2R is the preferential ribbon for the incorporation of Bi-surplus. Due to the high degree of ordering in the ribbons, it can be concluded that the alternation of Bi and As stabilizes the structure, and the presence of both elements in comparable amounts should be expected in vurroite. The surplus of Bi testifies, on the other hand, to a limited Bi/As solid solution behavior in the ribbons. It is probable that the solid solution extends also into the As-dominated compositions.

Organization of the lone electron pair micelles

The pyramidal ribbons of adjacent layers are interconnected by long M-S bonds. These weak interactions are influenced by the lone-electron pairs of As and Bi that are accommodated in the interlayer space, in the so-called lone-electron pair micelles (Fig. 7). The values of the long M^{3+}-S distances range between 2.875(12) and 3.665(9) Å. The distances close to the ends of a micelle are considerably shorter than those in the middle parts.

The lone-electron pair micelles are organized in zigzag layers of PbS-like rods (Fig. 7). The rods periodically meet after 1/2 *c*; the micelles are interrupted at these points.

TABLE 5. Coordination parameters* for the cation sites of vurroite

Atom/site	C.N.	<*d*>	d_{min}	d_{max}	V_s	ECC_V	SPH_V	V_p	υ	Valence†
Pb1	8	3.08(13)	2.881(11)	3.244(9)	123.248	0.1815	0.9629	51.4(4)	0.0375	2.00
Pb2	8	3.09(16)	2.883(9)	3.336(9)	123.896	0.2228	0.9668	51.8(4)	0.0360	2.02
Pb3	8	3.09(10)	2.883(13)	3.229(11)	123.543	0.1193	0.9396	51.9(4)	0.0314	1.94
Pb4	8	3.09(10)	2.954(12)	3.226(11)	124.013	0.1341	0.9458	52.0(4)	0.0322	1.91
Pb5	8	3.10(15)	2.918(12)	3.394(9)	124.983	0.1239	0.8761	51.8(4)	0.0434	1.94
Pb6	8	3.11(11)	2.942(11)	3.263(9)	125.454	0.0317	0.8914	51.9(4)	0.0456	1.86
Pb7	8	3.06(19)	2.836(7)	3.404(8)	119.349	0.2420	0.9346	48.7(4)	0.0588	2.21
Pb8	8	3.01(13)	2.886(7)	3.207(12)	114.588	0.1722	0.9556	47.3(3)	0.0473	2.41
Pb9	8	3.13(14)	2.988(13)	3.394(10)	128.420	0.1524	0.9067	53.9(4)	0.0324	1.75
Pb10	9	3.27(28)	2.809(9)	3.615(11)	144.713	0.3593	0.9178	69.3(5)	0.0183	1.66
Pb11	8	3.08(22)	2.752(12)	3.423(10)	124.228	0.1768	0.8263	50.4(3)	0.0647	2.16
Bi11	8	3.11(43)	2.637(11)	3.728(10)	124.225	0.4748	0.8263	50.4(3)	0.0646	2.68
As11	8	3.18(74)	2.293(10)	4.028(12)	124.224	0.7447	0.8263	50.4(3)	0.0646	2.01
Sn1a/Bi1b	6	2.62(19)	2.479(16)	2.878(11)	74.446	0.2589	0.8797	23.5(2)	0.0081	4.59
Sn2a/Bi2b	6	2.73(29)	2.492(13)	3.113(10)	83.513	0.3332	0.8003	25.9(2)	0.0271	3.82
Bi1	6	2.89(23)	2.613(8)	3.301(9)	103.801	0.3232	0.9635	30.5(2)	0.0776	2.72
As1	6	2.82(63)	2.188(11)	3.548(10)	105.167	0.7372	0.9313	29.5(2)	0.1197	3.21
Bi2	6	2.89(26)	2.623(8)	3.334(9)	105.918	0.3709	0.9543	30.9(2)	0.0831	2.88
As2	6	2.86(65)	2.232(11)	3.665(9)	107.657	0.7473	0.9566	30.6(2)	0.1068	3.01
As3a	6	2.75(45)	2.252(13)	3.191(14)	90.507	0.6052	0.9656	26.9(2)	0.0661	2.91
Bi3b	6	2.75(19)	2.526(12)	2.955(12)	90.508	0.2997	0.9656	26.9(2)	0.0661	
Bi4	6	2.82(23)	2.594(10)	3.102(9)	97.859	0.3488	0.9556	28.7(2)	0.0802	3.36
As5a	6	2.83(49)	2.323(29)	3.302(28)	101.268	0.6357	0.9884	29.8(2)	0.0761	3.12
Bi5b	6	2.83(40)	2.438(22)	3.259(13)	101.269	0.5531	0.9884	29.8(2)	0.0761	
Bi6	6	2.84(24)	2.548(8)	3.235(9)	99.304	0.3463	0.9833	30.0(2)	0.0525	3.17
As7a	6	2.75(45)	2.293(14)	3.185(14)	91.776	0.6121	0.9902	27.2(2)	0.0699	2.96
Bi7b	6	2.76(21)	2.484(14)	3.076(15)	91.776	0.3325	0.9902	27.2(2)	0.0699	
Bi8	6	2.83(23)	2.592(8)	3.062(11)	98.194	0.3439	0.9739	29.4(2)	0.0580	3.27

Notes: <*d*> = average bond distance, V_s = volume of the circumscribed sphere, ECC_V = volume eccentricity of the coordination, SPH_V = volume sphericity of the coordination, V_p = volume of the coordination polyhedron, υ = volume distortion.

* The polyhedron parameters for atomic coordinations are defined in Balić-Žunić and Makovicky (1996) and in Makovicky and Balić-Žunić (1998). All calculations done by IVTON (Balić-Žunić and Vicković 1996);

† Bond valence parameters of Brese and O'Keeffe (1991) used. For the mixed sites the calculated valences of individual species are multiplied by the fractional occupancies and summed.

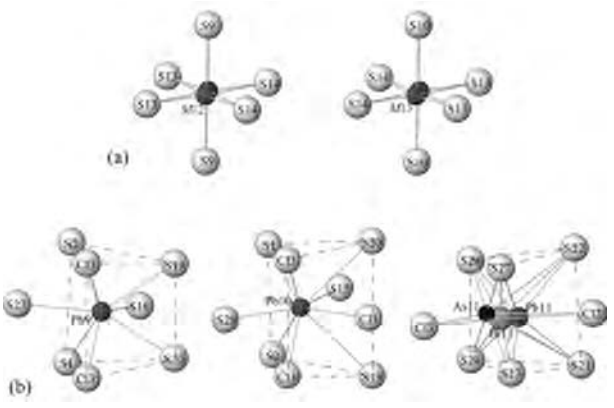

FIGURE 8. Coordination polyhedra in the crystal structure of vurroite. (**a**) Octahedral environment of mixed (Sn,Bi) sites; (**b**) from left to right: bicapped trigonal prismatic coordination of Pb9, tricapped trigonal prismatic coordination of Pb10, bicapped trigonal prismatic environment around the site 11.

One rod (D, Fig.7) is four atomic planes thick and three pyramids wide in its median plane. On (001) boundaries, it is limited by two opposing surfaces that display a pseudo-hexagonal motif of S atoms (H surfaces in Makovicky 1981). On the other two opposing sides Q surfaces occur (Q indicates a surface displaying a pseudo-tetragonal motif of sulfur atoms), truncated to the width of two square pyramids. On the H surfaces the D rods are connected by the lying bi-capped trigonal coordination prisms of M8 and M11.

The second kind of rod (C, Fig.7), is also four atomic planes thick, but two pyramids broad in the median plane, again with truncated Q and H surfaces. The connection on H surfaces of adjacent C rods is over the lying trigonal coordination prisms of M7.

Constricted layer portions

The constricted portions of layers are the narrow parts of (010) layers that connect the lozenge-shaped rods (Figs. 5 and 7). They consist of the two standing trigonal prisms Pb9 and Pb10, and the trigonal prism M11 occupied by Pb, Bi, and As atoms. Pb9 is a bi-capped trigonal prism and the two caps are S16 and S27 (Fig. 8); Pb10 is a tri-capped trigonal prism, with two caps that are sulfur atoms (S15 and S28) and third a chlorine atom (Cl1) (Fig.8).

The Pb-S distances in the trigonal prism Pb9 are of uniform length, while Pb10 shows one set of cation-to-ligand distances (S19 and S20) considerably longer than the others. The Cl3 atoms are shared by Pb9 and Pb10 (Figs. 5 and 7). A similar configuration is observed in dadsonite (Mumme and Makovicky, unpublished data in Makovicky 1993) and in the synthetic compounds $Pb_{12.65}Sb_{11.35}S_{28.35}Cl_{2.65}$ (Kostov and Macíček 1995) and $Pb_{4.32}Sb_{3.68}S_{8.68}Cl_{2.32}$ (Kostov et al. 1997).

The coordination of Bi11 is strongly asymmetric, with one set of M-S distances (Bi11-S21 and Bi11-S22) considerably longer than the other bonds of the prism (Fig. 8). The same is observed for As11 that binds via short bonds to four S atoms and a Cl atom, forming a pyramidal coordination, while showing very weak interactions with S21, S22, and Cl2. The atoms Cl2 and Cl3 are capping atoms in this coordination polyhedron; Cl3 is the closest cap for As11 and Bi11, while it is the farthest for Pb11. We consider it remarkable that the coordination pyramid of As11 has Cl as its

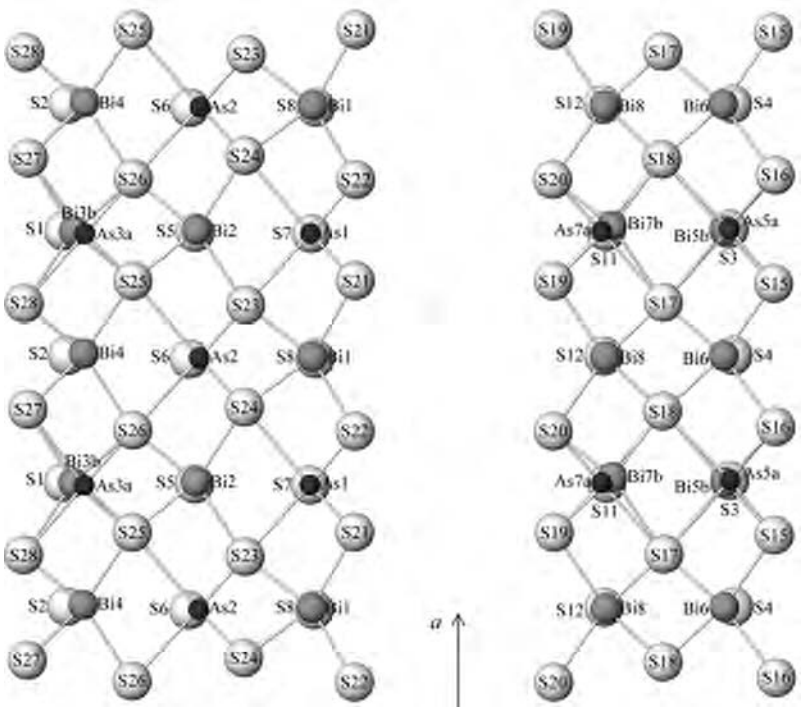

Figure 9. Trapezoidal ribbons of As and Bi atoms projected perpendicular to [100] and the planes of ribbons.

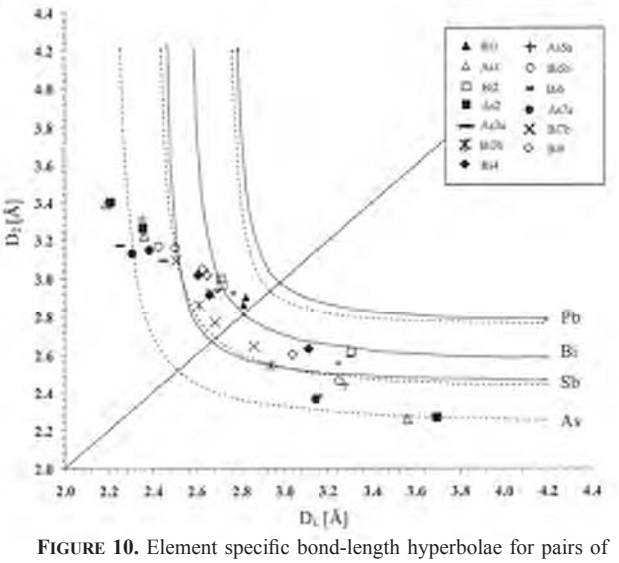

Figure 10. Element specific bond-length hyperbolae for pairs of opposing bonds (Berlepsch et al. 2001) with data for As and Bi cation positions belonging to the trapezoidal ribbons. Above the diagonal are bond-length ratios in the trapezoidal bases of the coordination pyramids, below the diagonal are the ratios of the distances to the pyramidal apex and to the S atom below the base of the pyramid.

vertex, as suggested by the results of bond-valence calculations. It is possible that Cl3 represents a mixed (Cl,S) site.

Crystal chemistry

Pb-Bi distribution

Because of the similarity in the scattering power of Pb and Bi, the distribution of these elements among the cation positions of vurroite cannot be derived from conventional diffraction measurements and has to be inferred on the basis of crystal-chemical considerations based on the refined bond-lengths (Table 5), the polyhedron volumes (V_p), the volume of circumscribed sphere (V_s), eccentricity (ECC), sphericity (SPH), and the degree of distortion (υ) of the coordination polyhedra. V_p, V_s, ECC, SPH, and υ were defined by Balić-Žunić and Makovicky (1996) and Makovicky and Balić-Žunić (1998), and their use in distinguishing Pb and Bi coordinations is discussed in Makovicky et al. (2001) and Berlepsch et al. (2001). The results of these calculations are summarized in Table 5. Analysis of coordination parameters for cations suggests that eight pure Pb sites (Pb1–Pb6, Pb9, and Pb10) are present in the structure of vurroite, whereas a mixed (Pb,Bi) occupancy is suggested for M7 and M8. Although both M7 and M8 show values of the shortest M-S distances similar to those of the other Pb sites, their coordination parameters differ from those of the other trigonal prismatic coordinated Pb sites. The coordination polyhedra around M7 and M8 show a degree of distortion (υ) slightly higher than those of the other Pb sites of the vurroite structure and, most indicative, they show the smallest values of V_p and V_s (Table 5). The latter are significantly lower than those observed in other structures of sulfosalts (see, e.g., Berlepsch et al. 2001) for polyhedra with the same coordination number and having Pb as a cation. The mixed (Pb,Bi) character of both M7 and M8 is finally confirmed by bond valence calculations (Brese and O'Keeffe 1991), which suggest the following distributions: 0.79 Pb and 0.21 Bi in M7; 0.59 Pb and 0.41 Bi in M8 (Table 5). This conclusion could not be confirmed by the values of eccentricity and the sphericity, but the latter two parameters oscillate strongly for all the polyhedra with CN8 of vurroite, without any clear trend. Finally, the occupancies obtained by the bond-valence calculations give the formula close to the one expected from the chemical

analysis (Garavelli et al. 2005) and their rounded values (0.80 Pb and 0.20 Bi in M7; 0.60 Pb and 0.40 Bi in M8) are accepted as those coming from the crystal structure parameters.

Final crystal-chemical formula

The crystal chemistry of vurroite is very complex, primarily due to the degree of cation substitutions (8 of the 23 cation sites show mixed character) and to the presence of variable amounts of chlorine in the structure. The analysis of the structure, supported by chemical evidence (Garavelli et al. 2005) suggests two main mechanisms of substitution, which act together, stabilizing the crystal structure. These two heterovalent substitutions can be defined as follows: $Pb^{2+} + Cl^{-} \leftrightarrow (Bi,As)^{3+} + S^{2-}$ and $Sn^{4+} + S^{2-} \leftrightarrow (Bi,As)^{3+} + Cl^{-}$.

The final structural formula of vurroite includes the following structural elements described in the preceding sections:

M(1–6,9,10); M(7,8); M(12,13); M11; M(14–23) and (S + Cl).

According to the occupancies reported in Table 2, the extended formula can be written as follows:

$Pb_{16}(Pb_{2.80}Bi_{1.20})_{\Sigma4}(Sn_{1.44}Bi_{0.56})_{\Sigma2}(As_{1.00}Bi_{0.60}Pb_{0.40})_{\Sigma2}(Bi_{11.58}As_{8.42})_{\Sigma20}(S_{54}Cl_{6})_{\Sigma60}$

or generally, taking in account the heterovalent substitutions:

$Pb_{16}(Pb_{x}Bi_{4-x})(Sn_{2-y}Bi_{y})(As_{2-z1-z2}Bi_{z2}Pb_{z1})(Bi,As)_{20}(S_{58-x-y-z1}Cl_{2+x+y+z1})$.

Evidently, the only way to obtain a chlorine-free composition would be to substitute some of the Pb sites in the first position in the formula partly or completely by Bi. As we have not observed such a tendency in the present crystal structure analysis, we consider this unlikely and conclude that Cl is a necessary constituent of vurroite.

Comparison to other structures

Synthetic $MnPb_{10}Sb_{12}S_{26}Cl_4O$

The synthetic compound $MnPb_{10}Sb_{12}S_{26}Cl_4O$ has been recently synthesized and its crystal structure determined by Doussier-Brochard (2006). The structure of this synthetic phase (Fig. 11) is characterized by lozenge-shaped composite rods very similar to those of the vurroite structure. In both structures, the lozenge-shaped rods consist of two triangular clusters of columns of base-sharing standing trigonal prisms [PbS_6] connected by a layer formed by a central octahedron flanked by two additional bicapped trigonal prisms (A; Fig. 11). The latter, however, are lying [$(Pb,Bi)S_6$] prisms in the structure of vurroite, whereas they are standing [$(Pb,Sb)S_6$] trigonal prisms in the synthetic $MnPb_{10}Sb_{12}S_{26}Cl_4O$. The central octahedrally coordinated site is occupied by Sn and Bi in vurroite and by Mn and Pb atoms in the synthetic phase. In both structures, the lozenge-shaped rods are surrounded by ribbons of trapezoidal coordination pyramids with thicknesses of two and three trapezoids. In the structure of vurroite, one 2R and one 3R element flank the opposite sides of lozenges. The rods formed with ribbons of adjacent lozenges have the structure of the PbS archetype (with As and Bi as cations). In the structure of $MnPb_{10}Sb_{12}S_{26}Cl_4O$, opposite sides of the lozenges are flanked by the same number of coordination pyramids. With the equivalent ribbons of adjacent lozenges they form two kinds of rods of SnS archetype having Sb as cation (B and C, respectively; Fig. 11).

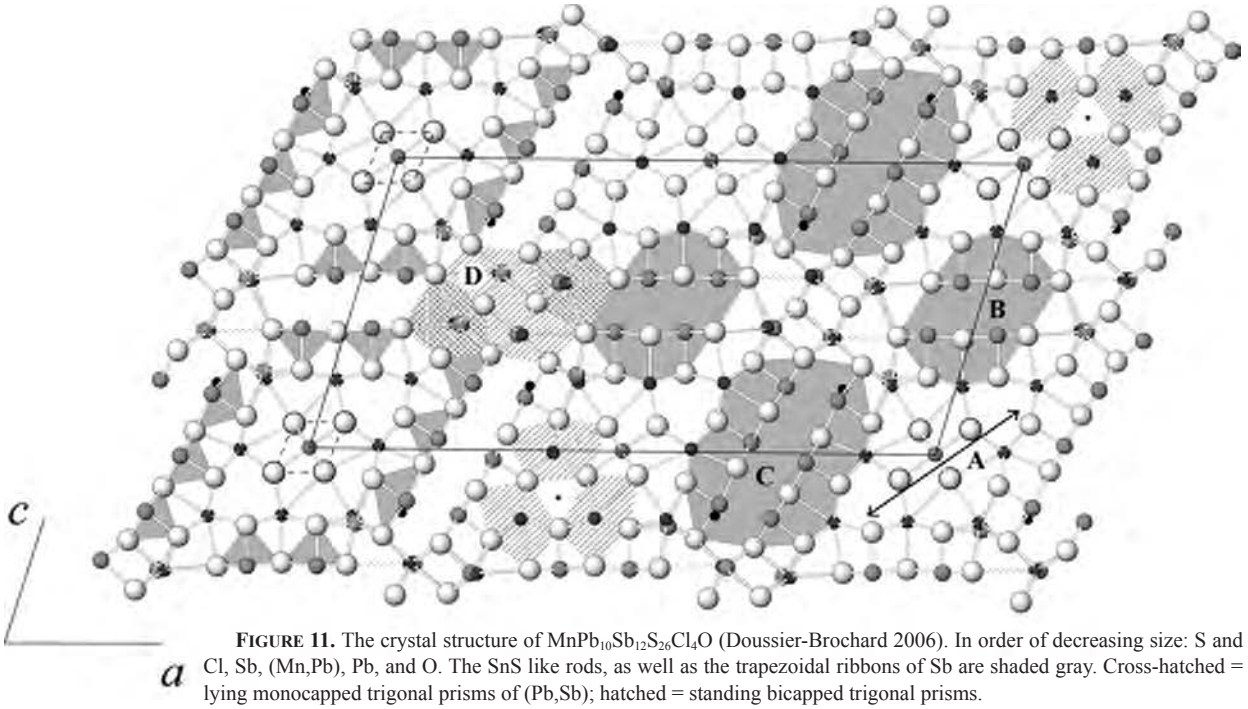

Figure 11. The crystal structure of $MnPb_{10}Sb_{12}S_{26}Cl_4O$ (Doussier-Brochard 2006). In order of decreasing size: S and Cl, Sb, (Mn,Pb), Pb, and O. The SnS like rods, as well as the trapezoidal ribbons of Sb are shaded gray. Cross-hatched = lying monocapped trigonal prisms of (Pb,Sb); hatched = standing bicapped trigonal prisms.

In the structure of vurroite, the lozenges are connected in layers by groups of three distinct cation sites showing trigonal prismatic coordination (the so-called constricted layer portion). The constricted layer portions in the structure of the synthetic phase $MnPb_{10}Sb_{12}S_{26}Cl_4O$ consist of four cation coordination polyhedra with a mixed (Pb,Sb) occupancy and representing, respectively, two lying monocapped and two standing bi-capped (mono-capped if the M-S bond at 3.77 Å is not considered) trigonal prisms (D; Fig. 11).

Zinckenite homologues

The threefold cluster of standing trigonal prisms of vurroite is also a characteristic element of the structures belonging to the zinckenite group (Makovicky 1985). In the crystal structure of zinckenite (Takeda and Horiuchi 1971; Portheine and Nowacki 1975; Lebas and Le Bihan 1976; Makovicky and Mumme 1983), which is the type structure of this family, three identical rods of galena-like structure surround each side of the triangular channels. These rods are four atomic planes thick and three half-octahedra wide. In vurroite, similar building blocks are present, however their configuration is altered and along two walls of a triangular channel the PbS-like blocks are reduced compared to those in zinckenite. On the third side of the channel, the D rod of vurroite shows a configuration almost identical to the galena-like rods of zinckenite. The principal difference can be appreciated in the organization of the lone electron pair micelles: according to Makovicky and Mumme (1983), the PbS-like portions of zinckenite contain large lone-electron pair micelles inside the layer and small, single-cation micelles outwardly oriented. In the D rods of vurroite, only the inward-oriented micelles of the large type can be observed.

In Figure 12, the similar portions of the structures of vurroite and zinckenite are outlined. Whereas the D rod and the two neighboring threefold clusters of trigonal prisms in vurroite (Fig. 7) correspond entirely to the elements in the structure of zinckenite, the C rod represents only a part of the similar element in zinckenite. In its continuation two octahedra of the zinckenite layer are missing and are replaced by a standing tri-capped trigonal prism of Pb.

Kirkiite

The crystal structure of kirkiite has been recently solved by Makovicky et al. (2006). They described this structure as a stacking sequence of three distorted octahedral layers interleaved by single trigonal prismatic layers or, alternatively, as composed of transitional SnS/PbS like layers twinned on $(210)_{SnS}/(111)_{PbS}$ by mirror reflection across the boundary layer of capped trigonal prisms.

In the structure of vurroite, topologically similar building blocks can be observed. They consist of the alternating sequence of the D rods and the couple of opposing lying trigonal prisms (M8 and the split site M11), which interconnect these rods on their (001) surfaces. The cross-hatched zone of Figure 13a indicates the structural portion of vurroite, which can be compared with the structure of kirkiite (Fig. 13b).

In the structure of kirkiite, the (111) PbS layers [parallel to kirkiite's (010) planes] are three octahedra thick; the octahedra in the marginal portions are largely distorted (they may also be described as split octahedra or lying mono-capped trigonal prisms). In the D rods of vurroite, which are three octahedra wide, no strong differences can be observed in the degree of their distortion. However, in the octahedra of vurroite, occupied by As and Bi, the four S atoms that form the equatorial plane show a more accentuated trapezoidal distortion compared to those in kirkiite, where the octahedra are primarily occupied by Pb.

In vurroite, the lying trigonal prisms M8 and M11 that interconnect the D rods, form a four-membered cluster around the capping Cl2 atoms and the two equivalent [100] rows (Fig. 14a). In kirkiite (Fig. 14b), only one row of paired trigonal prisms corresponds exactly to those of vurroite. The other row, which consists of alternating trigonal prisms of Pb and large trigonal prisms accommodating the statistically split As atoms, differs from vurroite rows both in the respective orientation of prisms and in their displacement relative to the first row.

The C rods of vurroite and the adjacent trigonal prisms M7, which interconnect these rods can be interpreted as a restricted kirkiite motif (hatched zones in Figure 13a), characterized by PbS slabs two octahedra wide and by only one lying trigonal prism between them.

Only a very small content of Cl has been registered in kirkiite (Pinto et al. 2006) and no specific Cl sites exist in this structure.

Box-work structures

According to Makovicky et al. (2001) the "box-work" structures are complex structures characterized by three (or

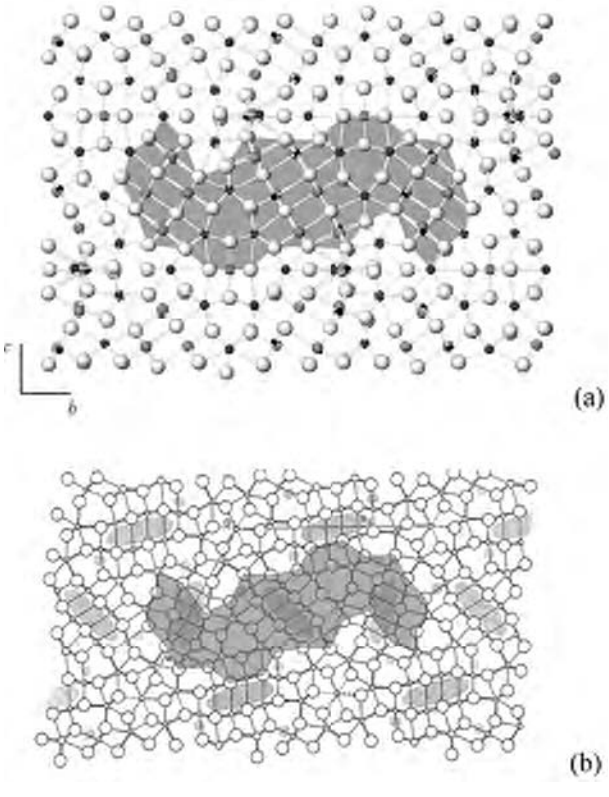

FIGURE 12. Comparison between the crystal structure of vurroite (**a**) and that of zinckenite (Portheine and Nowacki 1975; Lebas and Le Bihan 1976) (**b**). The similar portions in the two crystal structures are shaded in gray. Part **b** is modified from Makovicky and Mumme (1983).

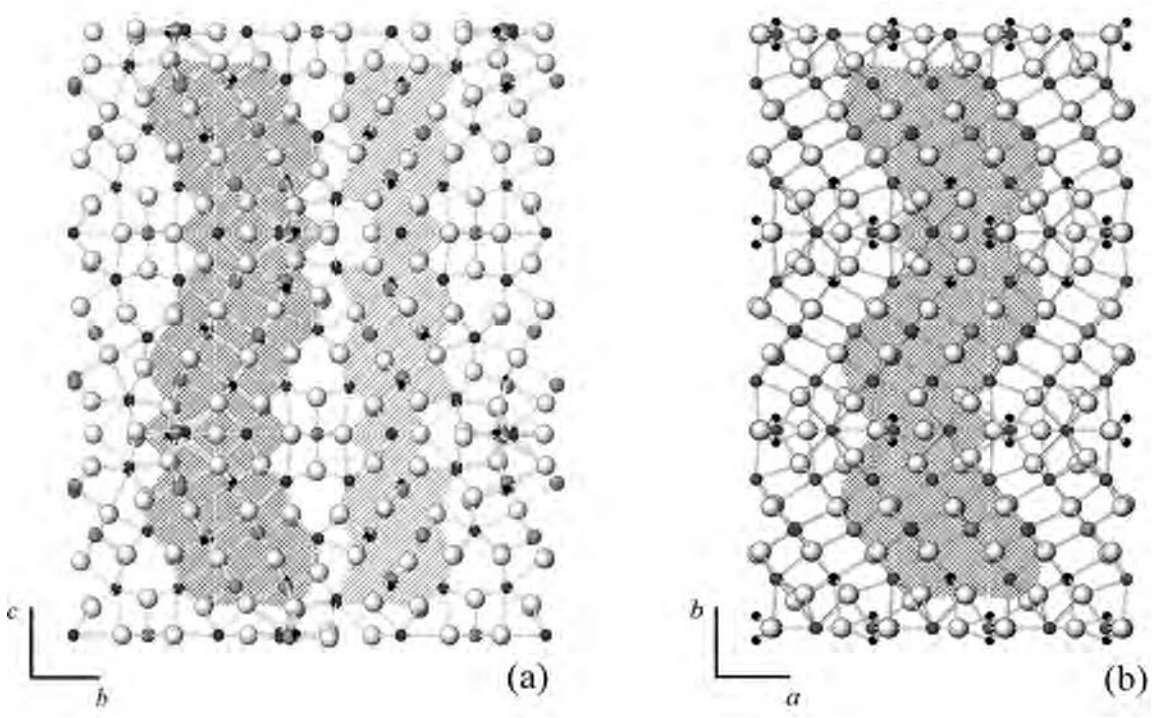

FIGURE 13. Comparison between the crystal structure of vurroite (**a**) and that of kirkiite (Makovicky et al. 2006) (**b**). Cross-hatched are the similar portions in the two crystal structures. Hatched portion in vurroite represents a restricted kirkiite-like motif.

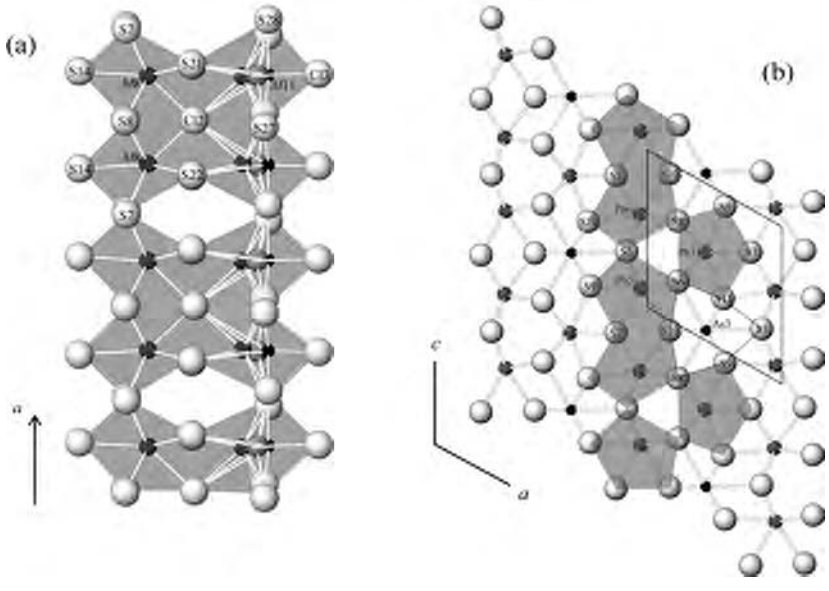

FIGURE 14. (**a**) Chains formed of four-member clusters of lying trigonal prisms of M8 and M11 in the crystal structure of vurroite; (**b**) corresponding chains of trigonal prisms of Pb and As in kirkiite. Only one row (with paired Pb trigonal prisms) corresponds exactly to those of vurroite, whereas the other row that consists of Pb trigonal prisms and large trigonal prisms accommodating two split As atoms assumes another configuration.

more) types of rod (layer) elements, two of which form a sort of box-work (honeycomb) arrangement accommodating the other elements. This results in two types of non-commensurate interfaces, in two sets that are oblique to each other. These structures differ significantly from all the other typical complex structures of sulfosalts, which have non-commensurate match on only one type of interface and consist of one or two types of rods (layers).

In this kind of structure, the joining of two distinct pseudo-tetragonal building-blocks usually creates a hole, which accommodates pseudo-hexagonal blocks. The main examples of this category are neyite (Makovicky et al. 2001), pillaite (Meerschaut et al. 2001) and the rare-earth sulfide $Er_9La_{10}S_{27}$ (Carré and Laruelle 1973).

The structure of vurroite can also be considered a box-work structure with the smallest possible pseudo-hexagonal block. It is the (Sn,Bi) octahedron in the center of the lozenge (Fig. 6). The same can be said about $MnPb_{10}Sb_{12}S_{26}Cl_4O$ (Doussier-Brochard 2006).

ACKNOWLEDGMENTS

This work is a part of the Ph.D. thesis by Daniela Pinto financed by F.S.E.—P.O.N. 2000–2006 "Ricerca Scientifica, Sviluppo Tecnologico ed Alta Formazione" Misura III.4—Formazione superiore e Universitaria. The authors are grateful to S. Merlino (University of Pisa) for his keen interest and valuable remarks, as well as for the critical reading of the manuscript. We are grateful to F. Vurro and A. Garavelli (University of Bari) for their helpful suggestions. The authors also thank L. Bindi (University of Florence) and the second anonymous referee for their careful and helpful reviews. Many thanks are also due to the Associate Editor P. Bonazzi for the helpful assistance. Financial support was provided by the University of Bari (Fondi di Ateneo 2006) and by the Danish Research Council of Natural Science, Project Number 21.03.05.19.

REFERENCES CITED

Balić-Žunić, T. and Makovicky, E. (1996) Determination of the Centroid or "the Best Centre" of a Coordination Polyhedron. Acta Crystallographica, B52, 78–81.

Balić-Žunić, T. and Vicković, I. (1996) IVTON—Program for the calculation of geometrical aspects of crystal structures and some crystal chemical applications. Journal of Applied Crystallography, 29, 305–306.

Berlepsch, P., Makovicky, E., and Balić-Žunić, T. (2001) The crystal chemistry of meneghinite homologues and related compounds. Neues Jahrbuch für Mineralogie-Monatshefte, 115–135.

Brese, N.E. and O'Keeffe, M. (1991) Bond-valence Parameters for Solids. Acta Crystallographica, B47, 192–197.

Carré, D. and Laruelle, P. (1973) Structure cristalline du sulfure d'erbium et de lanthane, $Er_9La_{10}S_{27}$. Acta Crystallographica, B29, 70.

Dornberger-Schiff, K. (1956) On the order-disorder (OD-structures). Acta Crystallographica, 9, 593.

——— (1959) On the nomenclature of the 80 plane group in three dimensions. Acta Crystallographica, 12, 173.

——— (1964) Grundzüge einer Theorie von OD-Strukturen aus Schichten. Abhandlungen der Deutschen Akademie der Wissenschaften zu Berlin. Klasse für Chemie, Geologie und Biologie, 3, 1–107.

——— (1966) Lehrgang über OD-Strukturen, 135 p. Akademie-Verlag, Berlin.

Dornberger-Schiff, K. and Fichtner, K. (1972) On the symmetry of OD-structures consisting of equivalent layers. Kristall und Technik, 7, 1035–1056.

Doussier-Brochard, C. (2006) Étude comparative de sulfures complexes naturels de fer au manganèse, et de leurs dérivés synthétiques. Cristallochimie et propriétés magnétiques, 218 p. Ph.D. thesis, Université de Nantes, France.

Ďurovič, S. (1997) Fundamentals of the OD theory. In S. Merlino, Ed., Modular Aspects of Minerals, 1, p. 3–28. EMU Notes in Mineralogy, Eötvös University Press, Budapest.

Evain, M., Petricek, V., Moëlo, Y., and Maurel, C. (2006) First (3 + 2)-dimensional superspace approach to the structure of levyclaudite-(Sb), a member of the cylindrite-type minerals. Acta Crystallographica, B62, 775–789.

Ferraris, G., Makovicky, E., and Merlino, S. (2004) Crystallography of modular materials. International Union of Crystallography Monographs on Crystallography no. 15, 370 p. Oxford Science Publications, U.K.

Garavelli, A., Mozgova, N.N., Orlandi, P., Bonaccorsi, E., Pinto, D., Moëlo, Y., and Borodaev, Y. (2005) Rare sulfosalts from Vulcano, Aeolian Islands, Italy. VI. Vurroite, $Pb_{20}Sn_2(Bi,As)_{22}S_{54}Cl_6$, a new mineral species. Canadian Mineralogist, 43, 703–711.

Guinier, A., Bokij, G.B., Boll-Dornberger, K., Cowley, J.M., Ďurovič, S., Jagodzinski, H., Krishna, P., de Wolf, P.M., Zvyagin, B.B., Cox, D.E., Goodman, P., Hahn, Th., Kuchitsu, K., and Abrahams, S.C. (1984) Nomenclature of Polytype Structures. Report of the International Union of Crystallography Ad-hoc Committee on the Nomenclature of Disordered, Modulated and Polytype Structures. Acta Crystallographica, A40, 399–404.

Kostov, V.V. and Macíček, J. (1995) Crystal structure of synthetic $Pb_{12.65}Sb_{11.35}S_{28.35}Cl_{2.65}$—A new view of the crystal chemistry of chlorine-bearing lead-antimony sulphosalts. European Journal of Mineralogy, 7, 1007–1018.

Kostov, V.V., Petrova, R., and Macíček, J. (1997) Crystal structure of synthetic $Pb_{4.32}Sb_{3.68}S_{8.68}Cl_{2.32}$. A chlorine-bearing alternative to $Pb_4Sb_4S_{11}$. European Journal of Mineralogy, 9, 1191–1197.

Lebas, G. and Le Bihan, M.T. (1976) Etude chimique et structurale d'un sulfure naturel: la zinckénite. Bullettin de la Societé Française de Mineralogie et de Cristallografie, 99, 351–360.

Makovicky, E. (1981) The building principles and classification of bismuth-lead sulphosalts and related compounds. Fortschritte der Mineralogie, 59, 137–190.

——— (1985) Cyclically twinned sulphosalt structures and their approximate analogues. Zeitschrift für Kristallographie, 173, 1–23.

——— (1993) Rod-based sulphosalt structures derived from the SnS and PbS archetypes. European Journal of Mineralogy, 5, 545–591.

Makovicky, E. and Balić-Žunić, T. (1998) New measure of distortion for Coordination Polyhedra. Acta Crystallographica, B54, 766–773.

Makovicky, E. and Mumme, W.G. (1983) The crystal structure of ramdohrite, $Pb_6Sb_{11}Ag_3S_{24}$, and its implications for the andorite group and zinckenite. Neues Jahrbuch für Mineralogie-Abhandlungen, 147, 58–79.

Makovicky, E., Balić-Žunić, T., and Topa D. (2001) The crystal structure of neyite, $Ag_2Cu_6Pb_{25}Bi_{26}S_{68}$. Canadian Mineralogist, 39, 1365–1376.

Makovicky, E., Balić-Žunić, T., Karanović, L., and Poleti, D. (2006) The crystal structure of kirkiite $Pb_{10}Bi_3As_3S_{19}$. Canadian Mineralogist, 44, 177–188.

Meerschaut, A., Palvadeau, P., Moëlo, Y., and Orlandi, P. (2001) Lead-antimony sulfosalts from Tuscany (Italy). IV. Crystal structure of pillaite, $Pb_9Sb_{10}S_{23}ClO_{0.5}$, an expanded monoclinic derivative of hexagonal $Bi(Bi_2S_3)_9I_3$, from the zinckenite group. European Journal of Mineralogy, 13, 779–790.

Merlino, S. (1997) OD approach in minerals: examples and applications. In S. Merlino Ed., Modular Aspects of Minerals, 1, p. 29–54. EMU Notes in Mineralogy, Eötvös University Press, Budapest.

Nespolo, M. and Ferraris, G. (2001) Effects of the stacking faults on the calculated electron density of mica polytypes—The Ďurovič effect. European Journal of Mineralogy, 13, 1035–1045.

Otwinowsky, Z. and Minor, W. (1997) Processing of X-ray diffraction data collected in oscillation mode. Methods in Enzymology, 276, 307–326.

Palosz, B. and Salje, E. (1989) Lattice parameters and spontaneous strain in AX_2 polytypes: CdI_2, PbI_2 SnS_2 and $SnSe_2$. Journal of Applied Crystallography, 22, 622–623.

Pinto, D., Balić-Žunić, T., Garavelli, A., Garbarono, C., Makovicky, E., and Vurro, F. (2006) First occurence of close-to-ideal kirkiite at Vulcano (Aeolian Islands, Italy): Chemical data and single-crystal X-ray study. European Journal of Mineralogy, 18, 393–401.

Portheine, J.C. and Nowacki, W. (1975) Refinement of the crystal structure of zinckenite, $Pb_6Sb_{14}S_{27}$. Zeitschrift für Kristallographie, 141, 79 – 96.

Sheldrick, G.M. (1997a) SHELXS-97. A program for automatic solution of crystal structures. University of Göttingen, Germany.

——— (1997b) SHELXL-97. A program for crystal structure refinement. University of Göttingen, Germany.

Takeda, H. and Horiuchi, H. (1971) Symbolic addition procedure applied to zinckenite structure determination. Journal of the Mineralogical Society of Japan, 10, 283–295.

MANUSCRIPT RECEIVED MARCH 16, 2007
MANUSCRIPT ACCEPTED DECEMBER 29, 2007
MANUSCRIPT HANDLED BY PAOLA BONAZZI